Article

The Influence of Parameters Affecting Mechanical Properties and Microstructures of Semi-Solid-Metal 7075 Aluminum Alloy by Using Friction Stir Spot Welding

Siva Sitthipong[1,a,*]**, Prawit Towatana**[1,3,b,*]**, Chaiyoot Meengam**[2,c,*]**, Suppachai Chainarong**[2] **and Prapas Muangjunburee**[4]

1 Marine and Coastal Resource Institute, Prince of Songkla University, Songkhla 90110, Thailand
2 Department of Engineering, Faculty of Industrial Technology, Songkhla Rajabhat University, Songkhla 90000, Thailand
3 Coastal Oceanography and Climate Change Research Center, Prince of Songkla University, Songkhla 90112, Thailand
4 Department of Mining and Materials Engineering, Faculty of Engineering, Prince of Songkla University, Songkhla, 90110, Thailand
E-mail: [a]Mechmat.s@gmail.com (Corresponding author), [b]Prawit.t@psu.ac.th (Corresponding author), [c]Chaiyoot.me@skru.ac.th (Corresponding author)

Abstract. This research aims to study the influence of parameters that affect the mechanical properties of semi-solid-metal 7075 aluminum alloy with friction stir spot welding process. The parameters for this experiment such as rotation welding speed at 380, 760, 1240 and 2500 rpm and welding time at 60, 90 and 120 seconds were employed respectively. The study found that the welded specimens at all the conditions can be welded very well. Moreover, friction stir spot welding process showed that the hardness in weld zone had an average value at 79.83 HV which is lower than the hardness of the base metal. The shear tensile strength of the welded specimens had the average value approximately 194.20 MPa at rotation welding speed of 2500 rpm, welding time of 90 seconds and plunge of depth of 2 millimetres. The microstructure in the weld zone and thermal mechanical affected zone were deformed permanently. Therefore, friction stir spot welding process of this aluminum alloy provided good effects on mechanical properties. Statistical analysis showed that the coefficient of determination R-square was equal to 93.50 percent. This means that the variations of the experiments were controllable, such as equipment or other factors in the experiment. For the remaining, only 6.50 percent was uncontrolled factors.

Keywords: SSM 7075 Aluminum alloy, friction stir spot welding, mechanical properties.

1. Introduction

The current welding technology is more diverse than ever since the different forms of products are manufactured to serve various types of industries. The choices of welding processes are also different and depend on the types of materials used, mechanical properties as well as the specimens for being welded. During the past 4 decades, solid state welding technique has been widely used [1], especially friction stir welding [2]. This interesting welding provides many advantages such as no filler adding, no melting, environmentally friendly process, etc [3]. However, friction welding technique is also available in many ways such as friction welding [4-6] or friction stir spot welding [7-9]. This interesting welding is applicable for welding parts of automobile and boat building industries[10]. Friction Stir Spot Welding (FSSW) was originally developed by friction stir welding at the Welding Institute in Great Britain [11]. The welded specimen relies on the heat derived from the friction of the surface of the specimen and tool shoulder. Then, the tool pin is employed to drag the soft heated material to be welded together. The significant variables of the FSSW are rotation welding speed, welding time and depth of plunge [12]. Furthermore, there are also other variables such as smoothness of surface, cleanliness of weld surface or even the shape of the welding tool [13-14]. However, most of the automobile and boat building industries usually use light weight material to produce the automotive and boat components or parts. Aluminum alloy is one of raw materials employed to manufacture parts and components since its light weight, high strength and corrosion resistance. Especially, Semi Solid Metal 7075 (SSM 7075) aluminum alloy is also used in automobile and boat building industries [15]. Thus, it is necessary to provide the best welding alloy or steel for manufacturing the premium grade products. For the aforementioned reasons, this led to the study of the influence of some relevant variables affecting mechanical properties and microstructure of SSM7075 aluminum alloy by using FSSW. The parameters included mechanical properties (strength, shear tensile strength and hardness) as well as microstructures. Then, the results were statistically analyzed to find the relationship between microstructures and mechanical properties of each variable in the experiments for determining the statistical reliability for engineering work.

2. Experimental Procedures

2.1. Semi-Solid-Metal 7075 Aluminum Alloy

The material used in this experiment was SSM 7075 aluminum alloy prepared through a squeeze casting process using semi–solid bubble casting technology known as "Gas Induce Semi Solid" or GISS. GISS technique will melt SSM7075 at the temperature of its semi-solid state. Then, inert gas will be sprayed through porous graphite bars to induce the circular flow of molten SSM 7075 alloy caused by gas reaction. This causes the molten alloy SSM 7075 to break down its dendrite structure into globular structure. Then, molten SSM 7075 aluminum alloy is poured into a square-shaped mold for casting with size of 100x100x20 mm (width x length x thickness). SSM 7075 aluminum alloy has good mechanical properties (corrosion resistance and light weight). It is used to produce the parts for aircrafts, automobiles and boats with the hardness of 99 HV and a tensile strength of 290 MPa, [16] and its chemical composition is shown in Table 1.

Table 1. Chemical composition of Semi-Solid-Metal 7075 Aluminum Alloy [16].

Materials	Zn	Mg	Cu	Fe	Si	Mn	Cr	Ti	Al
7075	6.08	2.5	1.93	0.46	0.4	0.03	0.19	0.02	Balance

2.2. The Preparation of Specimen for Friction Stir Spot Welding

The SSM 7075 aluminum alloy prepared by casting was cut by belt saw with cooling water for heat reduction to prevent a change in its microstructure. Then, the two cutting surface of the specimens were smoothened with a milling machine. The surface of specimens was resized to obtain the size of 28x95x4 mm (width x length x thickness) before testing as shown in Fig. 1. The totals of 96 specimens were used for this research. The experiments were designed for 4 replications with the experimental parameters including 4 rotation welding speeds and 3 different welding times.
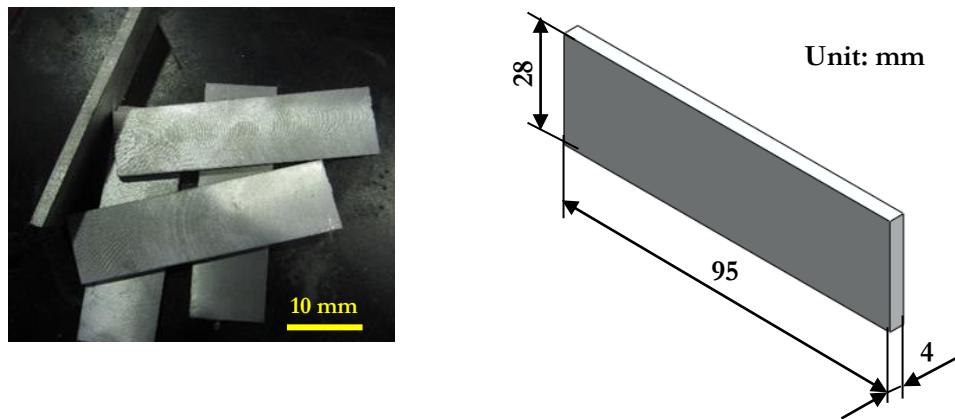
Fig. 1. The process of preparation SSM 7075 aluminum alloy for friction stir spot welding.

2.3. Variable and Experimental Design

The factors affecting the quality of welded joints are several. The main ones directly affecting the quality of welding are composed of shape of welding tool, rotation welding speed, the pressing force applied during welding and the type of material used to make the welding tool. However, in this research, we were interested in investigating the two controllable factors including the rotation welding speed and welding time which could affect mechanical properties of the welded specimens. The level of each factor was set as follows: 1) the rotation welding speeds were 380, 760, 1240, and 2500 rpm and 2) the welding times were 60 90 and 120 seconds. The fixed factor in the experiment was the shape of the welding tool. It had cylindrical shape and was made by iron with a shoulder size of 18 mm, diameter of 5 mm, a length of 6.2 mm and 28 mm length for lap joint welding (equal to the width of the specimen) with 2 mm depth of plunge.

2.4. Friction Stir Spot Welding Process

A milling machine was applied and modified for the FSSW by mounting and clamping the specimen to the milling machine base. Next, the pin tool was connected to transmission system of the milling machine. Then, variables were set according to experimental design. The experimental variables consisted of rotation welding speed of 380, 760, 1,240 and 2,500 rpm, depth of plunge of 2 mm and welding time of 60, 90 and 120 seconds respectively. Then, the welding tool was aligned to the center of the specimen as shown in Fig. 2. All the experiments were conducted at room temperature. Figure 2(a) illustrates the lap joint welding of the specimen with 28 mm overlap thickness by pressing the welding tool into the specimen surface at a uniform speed and pressure. Figure 2(b) shows the welding tool shoulder was pressed until plunging into the specimen at a depth of 2 mm. Meanwhile, the welding tool was rotating and being hold for certain time set by the experiment as shown in Fig. 2(c) to make the shoulder of the friction welding tool against the surface of the specimen. This caused the heat in the material under the shoulder and its sides, softened the material and created the alternate material flow from the force of rotation obtained from the welding tool. This behavior caused both pieces to stick together in solid state at the end of the holding time as shown in Fig. 2(d). The specimen after using FSSW had a groove (key hole) at the joint, which was caused by the tip of the welding tool.

Fig. 2.   The friction stir spot welding process.

2.5. Mechanical Testing

The specimens after FSSW were prepared with a milling machine for shear tensile strength test to determine the joint strength according to ASTM E384 standard [17]. This shear tensile strength testing was conducted by a pull speed of 1.67×10^2 mm/second at room temperature. For hardness testing, the specimens obtained from FSSW were cut until the weld areas were remained. The remain was mounted and the surface was smoothened with a lathe. Then, the specimens were test for Vickers Hardness with the Zwick/Roell model ZHU for the total hardness test of 31 spots around the weld area. The distance between testing spot was 0.2 mm apart. The applied pressure was 10 HV by using a pyramid square diamond head with an angle tip of 136 degrees and a holding time of 10 seconds.

2.6. Metallurgical Investigation

Some specimens after FSSW were subjected to microstructure inspection. They were polished with sand paper number 120, 380, 400, 600, 800, 1000 and 1200 respectively and finely polished by a flannel cloth with 5, 3 and 1 micrometer of particle size of aluminum powder. Then, the specimens were etched with Keller's reagent prior to investigate their microstructure by optical microscope (OM) and scanning electron microscope (SEM) in the area of microstructure changes.

3.   Result and Discussion

This work was to investigate the mechanical properties of SSM7075 aluminum alloy after FSSW with rotation welding speeds of 380, 760, 1,240 and 2,500 seconds, 2 mm depth of plunge and welding times of 60, 90 and 120 seconds. Then, the specimens were tested for mechanical properties and metal structures in order to analyze the variables affecting the welds. The results were as follows:

3.1. Characteristics of Microstructure after Welding

The FSSW of SSM 7075 aluminum alloy showed that the microstructure was different according to the different variables. Within the microstructure, the arrangement and density of each element were changed in weld zone and its surroundings due to the high temperature from friction that allow the each element to freely move based on its melting temperature. However, we were interested in investigating 5 positions of microstructure of the specimens after welding. These were the flash areas of the specimens after welding (position A and B) shown in Fig. 3. The interface between the upper and lower specimens that the specimens were attached (position C and D) and at the bottom of the specimen (position E). All the aforementioned positions were influenced by the heat from the welding resulting in the different structural changes occurring in the specimens as illustrated by positions of microstructural investigation in Fig. 3. For microscopic examination, a 200X magnification of microscope was employed. However, this study emphasized on only the microstructure at 1) the rotation welding speed of 2500 rpm and 90 second welding time and 2) the rotation welding speed of 1240 rpm and 60 second welding time since these variables provided the highest and lowest shear tensile strength in the experiments. For other variables in the experiments, the results of the microstructure experiments were consistent to the former ones.
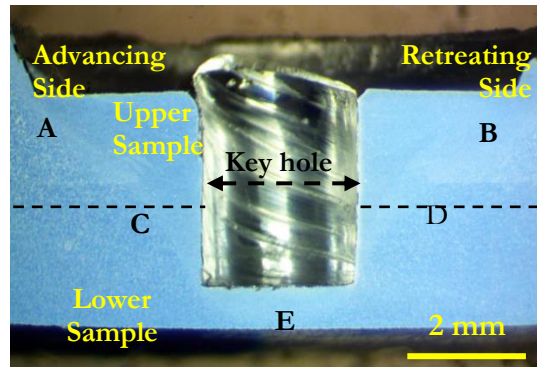
Fig. 3.   The positions of the specimen after welding for microstructure investigation.

The FSSW certainly resulted in altering the original globular structure of the material especially at the weld area and the tool pin which was affected by the heat during welding. This made the Eutectic Phase ($MgZn_2$) smaller from destruction by mechanical behavior until it could not be restored to its original shape. Changes in the $MgZn_2$ Phase could affect the mechanical properties of the specimens after welding. Figure 4 illustrates the microstructure in the areas of structural changes. The experiment was carried out at the rotation welding speed of 2500 rpm for 90 second welding time. The results showed that, in the stirred area, globular structure was altered to fine grains, which alternate between the $MgZn_2$ Phase and α-Al (Aluminum matrix Phase). However, the non-stirred area revealed that the grain size grew from the heat generated by the friction as shown in Fig. 4 (a and b). The grain growth mechanisms were caused by connecting smaller grain to the larger one and eventually lead to recrystallize the new one [18]. The new grain recrystallization after welding would occur alongside the stirred area. Moreover, between the upper and lower specimens could generate small long hooks. Heat and friction would get rid of the hooks [19] as illustrated in Fig. 4(c). The microstructure would show the coarse grain pattern in this area since the heat transferred from the upper specimen to the lower one. Therefore, there was not sufficient heat to alter the grain to the finer one as shown in Fig. 4(d). However, the heat generated during FSSW of SSM 7075 aluminum alloy also affected the microstructure changes at the end of the tool pin as shown in Fig. 4(e).

The results revealed that the microstructure was a fine grain structure around the tool pin and a coarse grain structure next to the tip of the tool pin [20]. From this investigation of microstructure at the weld area obtained from rotation welding speed of 2500 rpm and 90 second welding time, it showed no void or defect after the welding. This indicated that the aforementioned variables were appropriate in the welding. This would affect the mechanical properties in a good direction. Heat generated during FSSW is very important since the heat will lead to a change in microstructure and mechanical properties after the welding. Rotation welding speed is a variable that affects the change of heat as illustrated in the equation of FSSW below [21]:

$$Q = 4/3 \; \pi r^2 n \mu \varrho \omega R^3 \tag{1}$$

where Q is the heat value generated during the FSSW (heat input), n is the rotation welding speed, μ is the friction coefficient, and R is the radius of welding tool (Shoulder Radius). According to the above equation, increasing the rotation welding speed and increasing the radius of welding tool results in raising the heat during FSSW. Thus, the relationship between the rotation welding speed affecting the heat during the FSSW could be explained by the material flow in the weld zone. Many researchers have studied the heat model from FSSW. In addition, friction is another important variable affecting the heat as indicated by Coulomb's Theory below [22]:

$$q_f = F_f \, \upsilon \tag{2}$$

where q_f is Heat temperatures, F_f is friction force, and υ is the rotation welding speed (Pin Rotation). Furthermore, the calculation of υ can be calculated from $\upsilon = 2\pi r \mu n$ where n is the rotation welding speed, μ is the coefficient of friction between the tool and specimen and r is the size of stirring tool + the size of weld tool (Tool Pin + Toll Shoulder).
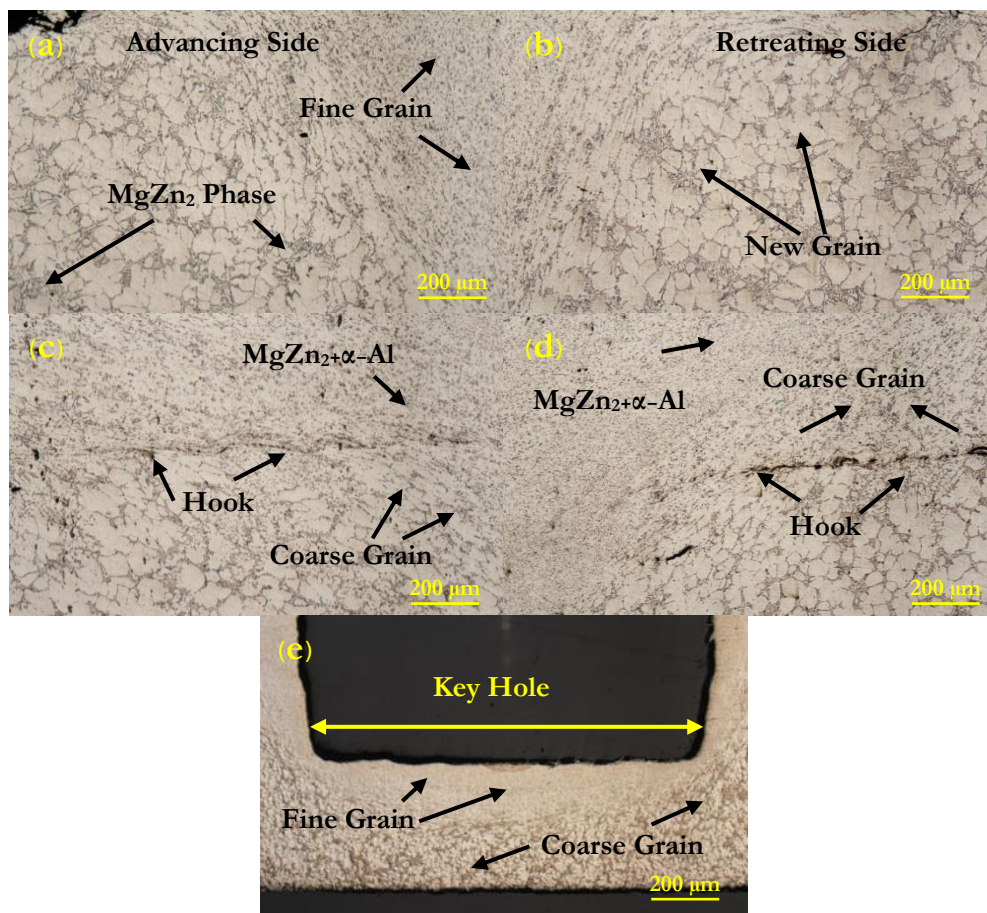
Fig. 4.   Characteristics of the weld zone structure at rotation welding speed of 2,500 rpm and 90 seconds of welding time.

This could be noticeable that at the rotation welding speed of 1,240 rpm with the welding time of 60 seconds had less microstructure changes than those of the microstructure at the rotation welding speed of 2,500 rpm with the welding time of 90 seconds (Fig. 5) since heat generating mechanism can hardly proceed from less rotation welding speed. It was noteworthy that the welded area had a narrow fine grain structure as shown in Fig. 5 (a and b). It was found that the α-Al phase had incomplete changes resulting in producing coarse grains and less MgZn$_2$ phase intrusion into the α-Al phase (Fig. 5 (c and d)), which was the joint area of the upper and lower specimens. It was found that there were big hooks on both sides of the specimens. This was caused by the heat during welding that could not be transferred to the welded area and; therefore, impossible to eliminate the hooks along the joints [23]. Similarly, less heat caused discontinuity of welding and led to poor mechanical properties as well.

However, it was found that the microstructure (at rotation welding speed of 1,240 rpm and 60 second welding time) around the end of the stirring tool (tool pin) had a narrow strip of fine grains adjacent to the tool, whereas the rest were coarse grains. This did not provide a good effect on the mechanical properties of the specimens after FSSW.
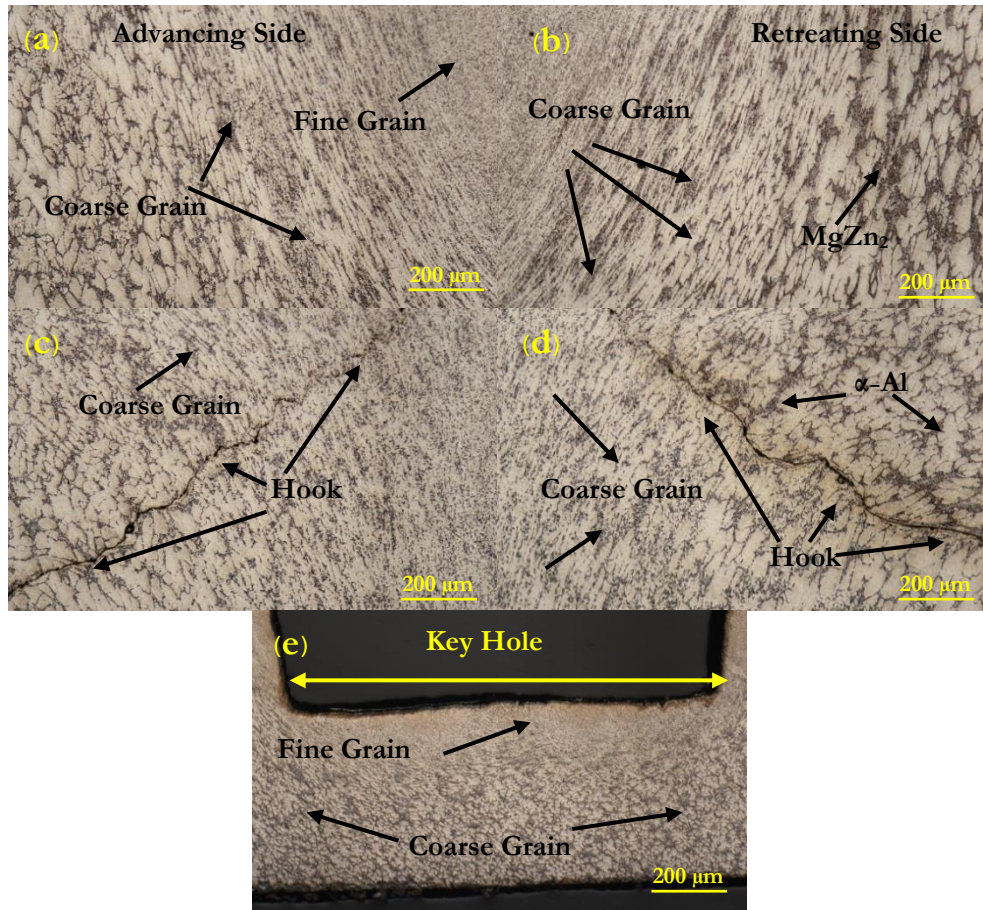
Fig. 5.   Characteristics of the weld zone structure at rotation welding speed of 1,240 rpm and 60 seconds of welding time.

3.2. Microstructural Investigation Results Using a Scanning Electron Microscope (SEM)

Figure 6 shows the microstructure of the weld area and the area adjacent to the weld obtained from SEM with 1,000x and 5,000x magnification respectively. Figure 6(a) illustrates the 1,000x magnification of $MgZn_2$ phase with the plate-like shape which is the original phase of material. The results showed that the $MgZn_2$ phase (ß-phase) (white) was intruded into the matrix of α-Al (α-phase) (gray) which looked like a spider web. However, heat influence caused the ß- phase to become fracture and deformation as ß′ -phase [24]. Heat transfer mechanism resulted in the disintegration of ß-phase into smaller sizes at the area which was influenced by heat from the variables at the rotation welding speed of 2,500 rpm and 90 second welding time. However, investigating the α-phase and ß-phase at rotation welding speed of 1,240 rpm and at 60 second welding time at 1,000x magnification revealed that the ß-phase was deformed to a small size spreading all over the weld zone and had been transformed by heat and friction to ß"-phase as shown in Fig. 6(c). It was noteworthy that there was a small gap in the α-phase as caused by the recrystallization of α-phase in the microstructure again [25]. This resulted in a very small gap (micro voids) intruded into the microstructure. Similarly, the 1,000x magnification image at rotation welding speed of 2,500 rpm and 90 second welding time exhibited the same direction as the rotation welding speed of 1,240 rpm and 60 second welding time did. It was noticeable that the higher rotation welding speed was employed, the finer size of ß"-phase and better distribution of ß"-phase all over the weld area occurred as compared to the rotation welding speed of 1,240 rpm and 60 second welding time (Fig. 6(d)). Figure 6 (e and f) shows the microstructure at the 500x enlargement which clearly shows the experimental results. It revealed that ß"-phase from the rotation welding speed of 2,500 rpm and welding rotation time of 90 seconds possessed small particle sizes and tiny gaps inserted among the α-phase, whereas the big particles of ß"-phase and large gaps were observed at 1,240 rpm rotation welding speed and 60 second welding time. The small ß"-

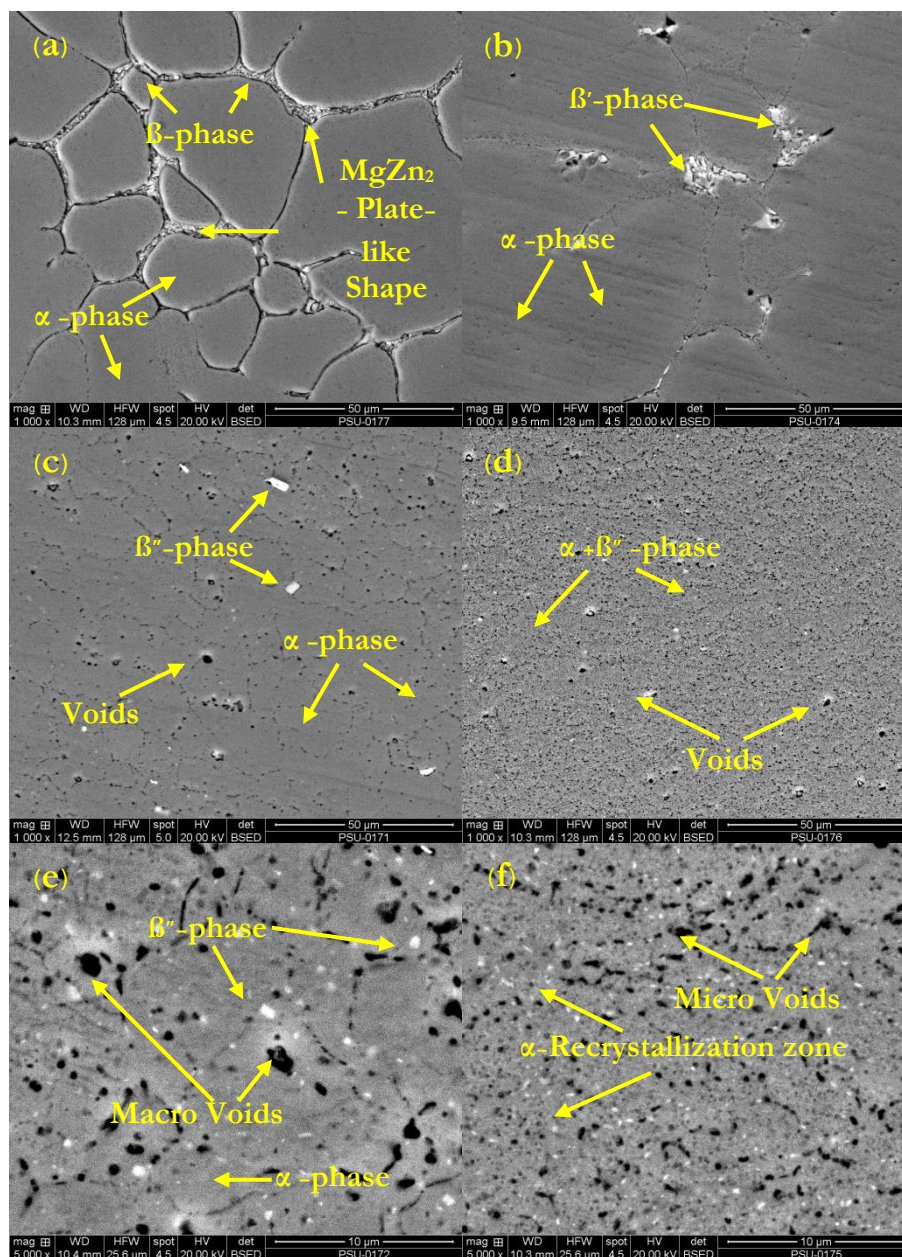phase strengthened the hardness of specimens, whereas the large void weakened the shear tensile strength as well [26].

Fig. 6.   Microstructure under scanning electron microscope.

3.3. Influence of Rotation Welding Speed Affecting the $MgZn_2$ Phase Size

The $MgZn_2$ phase particles were distributed into the matrix of SSM 7075 aluminum alloy in long plate shape with 43.17 micrometres long and 7.65 micrometres wide as shown in Fig. 6(a). After FSSW, the $MgZn_2$ phase particle size was smaller in the weld area attributed to heat and friction during welding process affecting the particle size of $MgZn_2$ phase. The $MgZn_2$ phase deformation mechanism was caused the heat making [27] the $MgZn_2$ phase to be soften while the force generated by the rotation caused the particles to fracture and break down to smaller sizes. However, the relationship between rotation welding speed and the phase size of $MgZn_2$ was shown in Fig. 7. In addition, the longer welding time it is, the more heat it is generated and dispersed which further allow elements to freely move. At 90 second welding time, the trend of $MgZn_2$ phase change revealed that at higher rotation welding speed was employed, the smaller particle size was obtained. At rotation welding speed of 380 rpm, the phase size of $MgZn_2$ was 7.54 micrometres wide and 44.2 micrometres long. When the rotation welding speed was increased from 760 to

2,500 rpm, the MgZn$_2$ phase was smaller with the length of 7.11, 4.62 and 3.79 micrometres and the width of 3.74, 3.56 and 2.17 micrometres respectively. The changes in the particle sizes would certainly affect the hardness and strength of specimens [28].
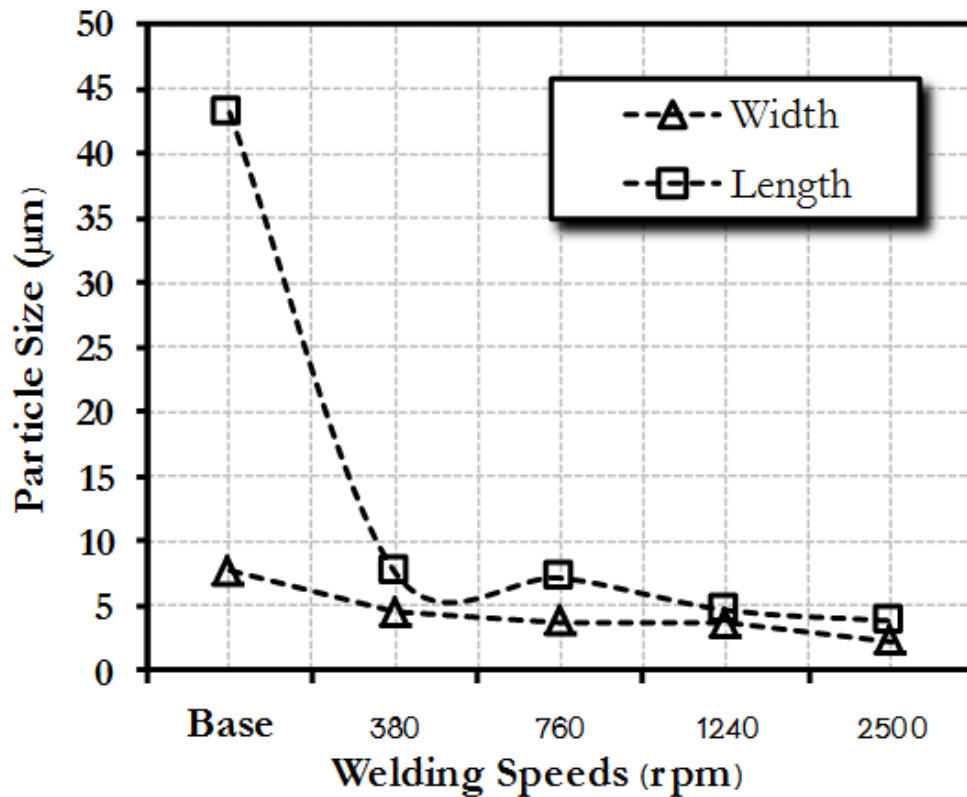

Fig. 7. The relationship between rotation welding speed and phase size of MgZn$_2$ at 90 seconds.

3.4. Shear Tensile Strength Test

For shear tensile strength test, the total of triplicate 64 samples were tested and analysed. Figure 8 shows the relationship between rotation welding speed and shear tensile strength at different welding time. The results revealed that the factors of the rotation welding speed and welding time affecting the change in shear tensile strength [29]. The longer welding time it is, the more heat it is generated and dispersed which further allow elements to freely move. At 90 seconds of welding time, it showed the best trend on shear tensile strength at all the rotation welding speed of FSSW. However, the welding time of 30 seconds was the shortest welding time resulting in insufficient heat to radiate throughout the weld area. Whereas, 120 second welding time generated the heat loss during rotation welding. The results indicated that the rotation welding speed of 2,500 rpm and 90 second welding time provided the highest average shear tensile strength of 190.24 MPa. On the contrary, the rotation welding speed of 1,240 rpm and the 60 second welding time gave the lowest average shear tensile strength of 103.05 MPa due to the voids at the weld area. The microstructure investigation revealed that the rotation welding speed of 1,240 rpm and 60 second welding time yielded bigger voids than those of the rotation welding speed of 2,500 rpm and 90 second welding time. The larger size and amounts of voids in the weld area could weaken the tensile properties by initiating cracks in the weld matrix and eventually resulting in fracture of welded specimens under tensile stress [30]. For comparison results, shear tensile strength values at rotation welding speed of 380 rpm and welding time of 60, 90 and 120 seconds gave the average shear tensile strength of 158.80, 183.80 and 103.88 MPa respectively. However, an increase in rotation welding speed at 760 rpm decreased in shear tensile strength with the average values of 146.35 and 108.47 MPa, except the 120 second welding time and had shear tensile strength of 132.04 MPa. At the rotation welding speed of 1,240 rpm, the shear tensile strength had better trend with shear tensile strength of 176.05 and 171.45 MPa. Furthermore, at the rotation welding speed of 2,500 rpm, it showed the good shear tensile strength with average values of 147.20 and 162.60

MPa at 60 and 120 second welding time respectively. However, the voids, residual stress, structural characteristics and other defects found after the FSSW could reduce the shear tensile strength of the specimens as well [31]. In every shear strength test, the failure occurred at the joint of the welding zone. All conditions were broken as a ductile characteristic.
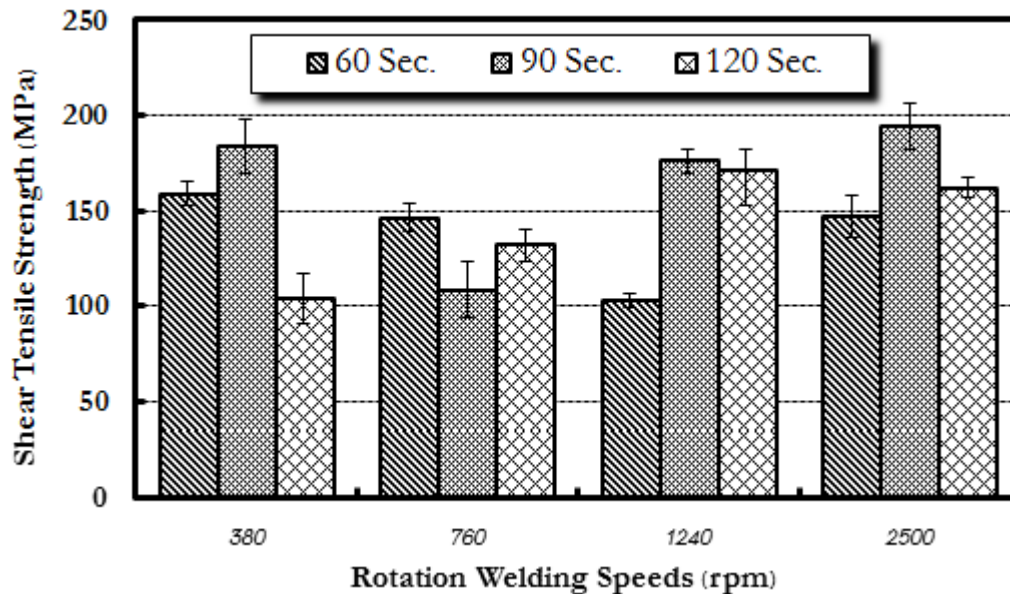

Fig. 8. The relationship among rotation welding speed at the shear tensile strength of 380, 760, 1,240 and 2,500 rpm and the welding time of 60, 90 and 120 seconds.

3.5. Analysis of Shear Tensile Strength Data Using Statistical Method Analysis of Model Accuracy

The analyses were carried out to determine data characteristic pattern including: randomness, straight line and distribution pattern around the zero (origin point) [32] to ensure the variability of the experimental conditions under controlled condition as follows: 1) Consider the independence of data by observing the graph of residual versus the order of the data to determine whether the data gave the random appear under controlled condition or not. Figure 9 showed no abnormality of graph line and; therefore, indicated that the data had random characteristic. 2) Consider whether distribution of the data possessing a normal distribution or not by observing more than 30 samples on the histogram of the residuals. Fig. 9. revealed that the data characteristic more closely resembled normal distribution. Thus, it could be concluded that the data was normal distribution. 3) Consider data around the origin point. The distribution pattern represented a similar trend with uniform variation around the origin point as illustrated in Fig. 9. From all the aforementioned consideration, it is suggested that the obtained data was reliable and could be employed to confirm the proposed hypothesis.

Analyses of shear tensile strength under various factors were carried out in Table 2. It was found that the main influence factors and complementary influence factors affecting the shear tensile strength since P-value =0.000 had less value than that of Alpha α =0.05. This supported that the complementary influence factors between the rotation welding speed and welding time affect shear tensile strength at the 95% confidence level with the similar trend as main influence factors did with the same confidence level (95%). This also supported the reliability of the data in the ANOVA table (Table 2) as well. Taking into consideration the coefficient of determination of R-square (R^2=93.50%), it can be implied that the variables of experimental parameters such as welding tool, rotation welding speed, welding time, depth of plunge etc. were controllable and; therefore, it gave the high value of R^2 =93.50%. On the other hand, the rest of 6.50 % was caused by uncontrolled factors and thus, the experimental design was acceptable.
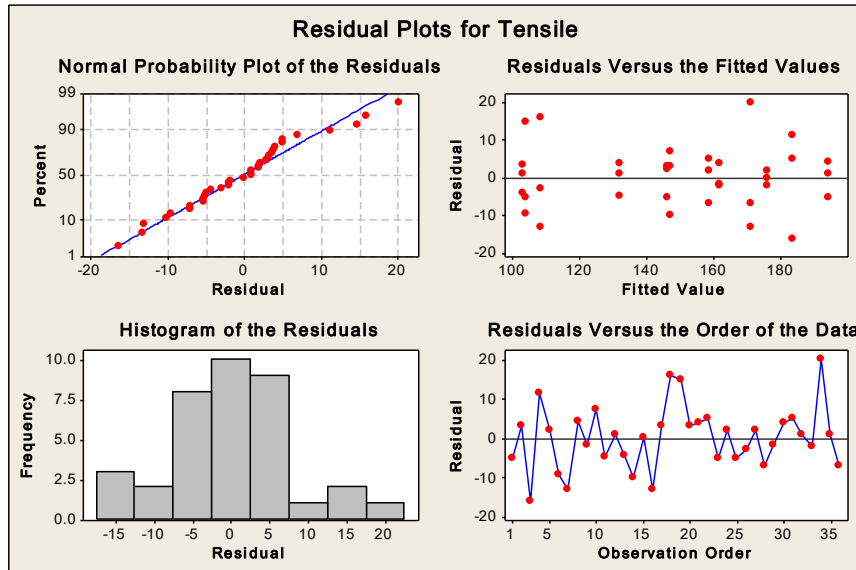
Fig. 9.   Analyses of reliability of the data and experimental model.

Table 2.   Analysis of variance (ANOVA) for the relationship between rotation welding speed and welding time.

Analysis of Variance for Shear Tensile Strength, using Adjusted SS for Tests						
Source	DF	Seq SS	Adj SS	Adj MS	F	P
Rotation Welding Speeds	3	6824.1	6824.1	2274.7	24.24	0.00
Welding Time	2	5094.7	5094.7	2547.4	27.15	0.00
Rotation Welding Speeds *Welding Time	6	20483.9	20483.9	3414	36.38	0.00
Error	24	2252.1	2252.1	93.8		
Total	35	34654.8				

S = 9.68705   R-Sq = 93.50 %   R-Sq(adj) = 90.52 %

3.6. Hardness Test

The hardness testing of SSM 7075 aluminum alloy obtained from the FSSW by measuring of the hardness of 31 positions with the distance between each testing position of 200 micrometers (0.2 mm) was conducted. Vickers Hardness Test was employed with the press force of 10 grams and for 10 seconds (HV_{10}) to measure the hardness in the Weld Zone (WZ), Thermals mechanical affecting zone (TMAZ) and original Base Metal (BM) at the rotation welding speed of 2,500 rpm, welding time of 90 seconds and 2 mm depth of plunge. Figure 10 showing the result of the hardness test revealed that the zone affected by the heat from the welding changed its hardness especially in the zone obtained the heat from tool shoulder resulting in significantly increasing hardness [33]. However, the mechanism of hardness change around the welding zone from FSSW was also caused by density of the alloy after stirring, cooling rate after welding, residual stress and the change of heat during the welding [34]. The highest hardness obtained from the test had the average value of 79.83 HV in the weld zone and 115.18 HV in the heat affected zone, whereas the original of SSM 7075 aluminum alloy had the average value of 99 HV. Similarly, the results of FSSW test for other variables had the same aforementioned trend especially the heat affected zone possessed the higher average hardness than those of the weld zone and the original texture of base material. The FSSW is based on the heat generation in the solid state. Hence, welding variables are important key parameters since the heat occurring will affect the change in the microstructure leading to different hardness and mechanical properties of welding parts as well.
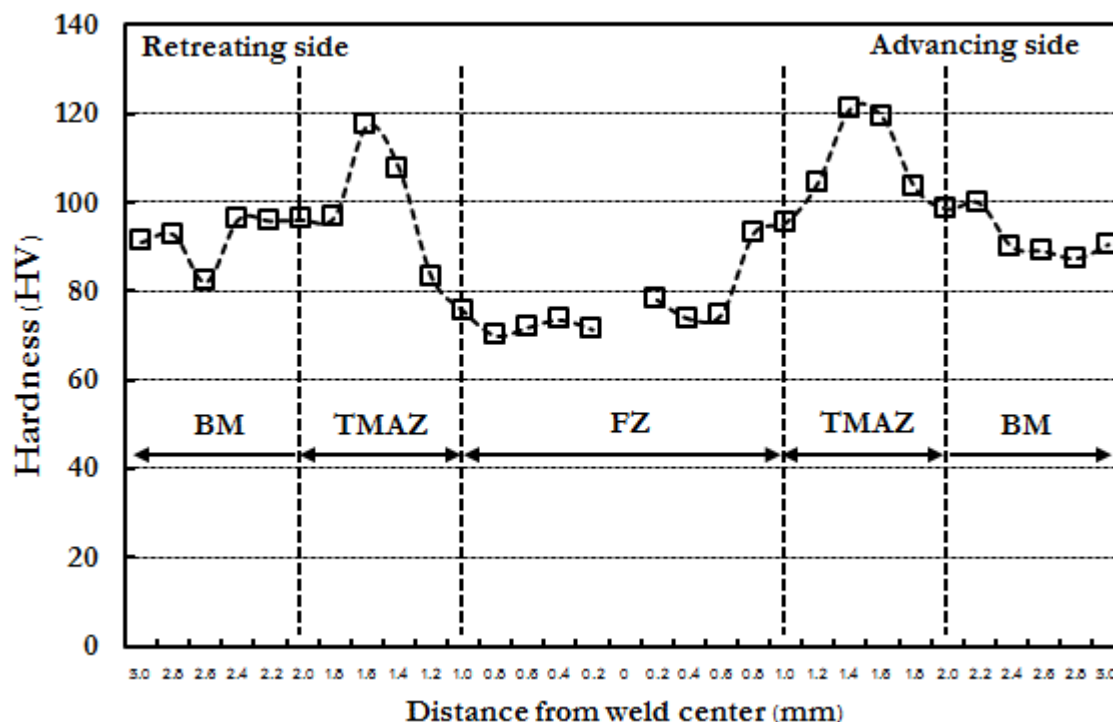
Fig. 10. Hardness values of the welded specimens at rotation welding speed of 2,500 rpm and welding time of 90 seconds.

4. Conclusion

The experimental results of FSSW Test of SSM 7075 aluminum alloy were satisfying. The good results were obtained from both hardness and shear tensile strength tests. Both microstructure and qualitative investigation could be concluded as follows:

Experiment for determining the suitable variables of FSSW for the SSM 7075 aluminum alloy reveals that the suitable rotation welding speed of 2,500 rpm, welding time of 90 seconds could provide the maximum value of the shear tensile strength at 194.20 MPa and highest hardness at 79.83 HV in the weld zone. The microstructure in the eutectic weld zone was changed from $MgZn_2$-ß-phase (original phase) to $MgZn_2$-ß''-phase caused by the friction and heat generated during welding. Furthermore, the α-phase aluminum matrix was recrystallized caused by the combination of the α- ß''-phase from the material flow circulation and there were micro voids intruding within the weld zone as well. Moreover, the rotation welding speed affected the change of phase size of $MgZn_2$. At the rotation welding speed of 2,500 rpm and welding time of 90 seconds, it yielded the smallest particle size at 3.79 micrometres long and 2.1 micrometres wide respectively. Analysis of the data obtained from shear tensile strength test under the various factors revealed that the determination coefficient of R-square (R^2) of 93.50% implied that the variables of experimental parameters such as welding tool, rotation welding speed, welding time, depth of plunge etc. were controllable whereas the rest of 6.50% was caused by the various uncontrollable factors. Thus, this experimental design could be acceptable.

Acknowledgements

References

[1] X. W. Yang, T. Fu, and W. Y. Li, "Friction stir spot welding: A review on joint macro and microstructure, property, and process modelling," *Advances in Materials Science and Engineering*, vol. 2014, pp. 1-11, 2014.

[2] N. T. Kumbhar and K. Bhanumurthy, "Friction stir welding of Al 5052 with Al 6061 alloys," *Journal of Metallurgy*, vol. 2012, pp. 1–7, 2012.

[3] N. Martinez, N. Kumar, R. S. Mishra, K. J. Doherty, "Microstructural variation due to heat gradient of a thick friction stir welded aluminum 7449 alloy," *Journal of Alloys and Compounds*, vol. 713, pp. 51–56, 2017.

[4] H. Khalid Rafi, G. D. Janaki Ram, G. Phanikumar, and K. Prasad Rao, "Microstructure and tensile properties of friction welded aluminum alloy AA7075-T6," *Materials and Design*, vol. 31, pp. 2375–2380, 2010.

[5] M. B. Uday and M. N. Ahmad-Fauzi, "Joint properties of friction welded 6061 aluminum alloy/YSZ–alumina composite at low rotational speed," *Materials and Design*, vol. 59, pp. 76–84, 2014.

[6] I.-D. Park, C.-T. Lee, H.-S. Kim, W.-J. Choi, and M.-C. Kang, "Structural considerations in friction welding of hybrid Al_2O_3-reinforced aluminum composites," *Transactions of Nonferrous Metals Society of China*, vol. 21, pp. s41–s46, 2011.

[7] G. D. Urso, "Thermo-mechanical characterization of friction stir spot welded AA6060 sheets: Experimental and FEM analysis," *Journal of Manufacturing Processes*, vol. 17, pp. 108–119, 2015.

[8] J. Gonçalves, J. F. dos Santos, L. B. Canto, and S. T. Amancio-Filho, "Friction spot welding of carbon fiber-reinforced polyamide 66 laminate," *Materials Letters*, vol. 159, pp. 506–509, 2015.

[9] E. Fereiduni, M. Movahedi, and A. H. Kokabi, "Aluminum/steel joints made by an alternative friction stir spot welding process," *Journal of Materials Processing Technology*, vol. 224, pp. 1–10, 2015.

[10] C. Connolly, "Friction spot joining in aluminium car bodies," *Industrial Robot: An International Journal*, vol. 34, pp. 17, 2007.

[11] M. Bevilacquaa, F. E. Ciarapicaa, A. D'Orazioa, A. Forcellesea, and M. Simoncini, "Sustainability analysis of friction stir welding of AA5754 sheets," *Procedia CIRP*, vol. 62, pp. 529–534, 2017.

[12] H. M. Rao, W. Yuan, and H. Badarinarayan, "Effect of process parameters on mechanical properties of friction stir spot welded magnesium to aluminum alloys," *Materials and Design*, vol. 66, pp. 235–245, 2015.

[13] Y. C. Chen, S. F. Liu, D. Bakavos, and P. B. Prangnell, "The effect of a paint bake treatment on joint performance in friction stir spot welding AA6111-T4 sheet using a pinless tool," *Materials Chemistry and Physics*, vol. 141, pp. 768–775, 2013.

[14] T. Hartman, M. P. Miles, S. T. Hong, R. Steel, and S. Kelly, "Effect of PCBN tool grade on joint strength and tool life in friction stir spot welded DP 980 steel," *Wear*, vol. 328-329, pp. 531–536, 2015.

[15] R. Meshkabadi, G. Faraji, A. Javdani, and V. Pouyafar, "Combined effects of ECAP and subsequent heating parameters on semi-solid microstructure of 7075 aluminum alloy," *Transactions of Nonferrous Metals Society of China*, vol. 26, pp. 3091–3101, 2016.

[16] C. Meengam, S. Chainarong, and P. Muangjunburee, "Friction welding of semi-solid metal 7075 Aluminum Alloy," *Materials Today: Proceedings*, vol. 4, no. 2, pp. 1303-1311, 2017.

[17] J. M. Piccini and H. G. Svoboda, "Effect of pin length on Friction Stir Spot Welding (FSSW) of dissimilar Aluminum-Steel joints," *Procedia Materials Science*, vol. 9, pp. 504-513, 2015.

[18] Y. F. Sun, H. Fujii, N. Takaki, and Y. Okitsu, "Microstructure and mechanical properties of dissimilar Al alloy/steel joints prepared by a flat spot friction stir welding technique," *Materials and Design*, vol. 47, pp. 350–357, 2013.

[19] W. Li, J. Li, Z. Zhang, D. Gao, W. Wang, and C. Dong, "Improving mechanical properties of pinless friction stir spot welded joints by eliminating hook defect," *Materials and Design*, vol. 62, pp. 247-254, 2014.

[20] Y. Tozaki, Y. Uematsu, and K. Tokaji, "A newly developed tool without probe for friction stir spot welding and its performance," *Journal of Materials Processing Technology*, vol. 210, pp. 844-851, 2010.

[21] W. Yuan, "Friction stir spot welding of aluminum alloys," master's thesis, Missouri University of Science and Technology, 2008.

[22] R. Mishra, P. S. De, and K. Nilesh, *Friction Stir Welding and Processing*. Switzerland: Springer International Publishing, 2014.

[23] J. Y. Cao, M. Wang, L. Kong, and L. J. Guo, "Hook formation and mechanical properties of friction spot welding in alloy 6061-T6," *Journal of Materials Processing Technology*, vol. 230, pp. 254-262, 2016.

[24] H. Dong, S. Chen, Y. Song, X. Guo, X. S. Zhang, and Z. Sun, "Refilled friction stir spot welding of aluminum alloy to galvanized steel sheets," *Materials and Design*, vol. 94, pp. 457-466, 2016.

[25] W. Yuan, R. S. Mishra, B. Carlson, R. Verma, and R. K. Mishra, "Material flow and microstructural evolution during friction stir spot welding of AZ31 magnesium alloy," *Materials Science and Engineering A*, vol. 543, pp. 200-209, 2012.

[26] C. Gao, R. Gao, and Y. Ma, "Microstructure and mechanical properties of friction spot welding aluminium–lithium 2A97 alloy," *Materials and Design*, vol. 83, pp. 719-727, 2015.

[27] R. Burapa, S. Janudom, T. Chucheep, R. Canyook, and J. Wannasin, "Effects of primary phase morphology on mechanical properties of Al-Si-Mg-Fe alloy in semi-solid slurry casting process," *Transactions of Nonferrous Metals Society of China*, vol. 20, pp. s857–s861, 2010.

[28] S. Venukumar, S. Yalagi, and S. Muthukumaran, "Comparison of microstructure and mechanical properties of conventional and refilled friction stir spot welds in AA 6061-T6 using filler plate," *Transactions of Nonferrous Metals Society of China*, vol. 23, pp. 2833–2842, 2013.

[29] S. H. Chowdhury, D. L. Chen, S. D. Bhole, X. Cao, and P. Wanjara, "Lap shear strength and fatigue life of friction stir spot welded AZ31 magnesium and 5754 aluminum alloys," *Materials Science and Engineering A*, vol. 556, pp. 500-509, 2012.

[30] Y. C. Chen, A. Gholinia, and P. B. Prangnell, "Interface structure and bonding in abrasion circle friction stir spot welding: A novel approach for rapid welding aluminium alloy to steel automotive sheet," *Materials Chemistry and Physics*, vol. 134, pp. 459-463, 2012.

[31] Y.-Ch. Lin and J.-N. Chen, "Influence of process parameters on friction stir spot welded aluminum joints by various threaded tools," *Journal of Materials Processing Technology*, vol. 225, pp. 347-356, 2015.

[32] D. C. Montgomery, *Designing and Analysis of Experiments*, 5th ed. New York: John Wiley & Sons, 2000.

[33] A. H. Plaine, U. F. H. Suhuddin, C. R. M. Afonso, N. G. Alcantara, and J. F. dos Santos, "Interface formation and properties of friction spot welded joints of AA5754 and Ti6Al4V alloys," *Materials and Design*, vol. 93, pp. 224-231, 2016.

[34] H. Liu, Y. Zhao, X. Su, L. Yu, and J. Hou, "Microstructural characteristics and mechanical properties of friction stir spot welded 2A12-T4 aluminum alloy," *Advances in Materials Science and Engineering*, vol. 2013, pp. 1-10, 2013.